Photodissociation of Ozone in the K Edge Region

T. Gejo,* K. Okada,† and T. Ibuki‡

Institute for Molecular Science, Okazaki 444-8585, Japan

N. Saito

Electro technical Laboratory, Umezono, Tsukuba-shi 305-0045, Japan

Received: February 8, 1999; In Final Form: April 16, 1999

Dissociative dynamics of the K shell excited ozone has been investigated by time-of-flight (TOF) mass spectra of fragment ions for the first time. The TOF spectra were acquired at 0 and 90° relative to the electric vector of linearly polarized soft X-ray. In the K shell excitation at the 529 eV photoabsorption peak, the energetic O^+ fragment ion was ejected anisotropically, while at the 536 eV band it was isotropic. The β values calculated from simulation of the TOF spectra are consistent with the previous assignments that the 529 eV band is the $\pi^* \leftarrow O_T(1s)$ resonance excitation and that the 536 eV band mainly consists of two transitions, $\pi^*(2b_1) \leftarrow O_C(1s)$ and $\sigma^*(7a_1) \leftarrow O_T(1s)$ [Gejo et al. *Chem. Phys. Lett.* 277 (1997) 497]. The TOF spectra show that the π^* excitation of terminal oxygen atoms generates more O_2^+ fragment than the excitation of the center oxygen atom.

1. Introduction

The inner-shell excitation of different atoms in a molecule leads to significantly different photodissociation pathways.[1−5] This effect is called site-specific dependence of fragmentation and has been observed in the K edge excitations of N_2O,[2] CF_3-CH_3,[3,4] CF_2CH_2,[4] BF_3,[5] and OCS.[6] In view of this, it is of interest to investigate the dissociation of ozone in the K shell excited state. We have previously observed two distinct peaks around 529 and 536 eV in the ion yield spectra of ozone.[7] The first peak at 529 eV has been assigned as the $\pi^*(2b_1) \leftarrow O_T(1s)$ resonance transition of the terminal oxygen atom and the second around 536 eV as the excitation to the π^* level from the center O(1s).[7] However, the latter has a wide bandwidth. We had performed the molecular orbital (MO) calculations on the basis of the SCF approximation and have been deconvoluted this band by two components: The calculation shows that one is the π^*-$(2b_1) \leftarrow O_C(1s)$ transition, as we expected, and another is the $\sigma^*(7a_1) \leftarrow O_T(1s)$ transition,[7] where the O_C and O_T mean the terminal and center oxygen atoms, respectively. The excitation from these different 1s levels of ozone is expected to give different photodissociation or ionization pathways.

The time-of-flight (TOF) spectra measurement is a useful tool for investigating the pathway of ionic fragmentation of a molecule.[8−10] In addition to this, angle-resolved measurement using the TOF apparatus provides information about the electronic state of the decomposing molecule:[11,12] The dipole transition probability depends on the molecular orientation with respect to the electric vector of polarized light. The Auger decay or autoionization process occurs within 10^{-14} s in the K shell excited molecule, while the rotational period of the molecule is longer than 10^{-13} s. Hence the initial memory of the innermost core excited molecule may not be faded in fragmentation.

* Corresponding author. Tel: +81-564-55-7403. Fax: +81-564-54-7079. E-mail: gejo@ims.ac.jp.

† Present address: Department of Chemistry, Faculty of Science, Hiroshima University, Higashi-Hiroshima 739-8526, Japan.

‡ Present address: Kyoto University of Education, Kyoto 612-8522, Japan.

In this paper, we report the angle-resolved TOF mass spectra of photofragment ions formed through the core-excitation of ozone. First we show the fragment distribution of ozone measured by TOF spectroscopy. Second we show the TOF distribution of the energetic fragments.

2. Experiment

Experiments were performed on the BL8B1 beamline at the UVSOR facility of the Institute for Molecular Science (IMS). Synchrotron radiation (SR) was monochromated by using a 15-m constant-deviation grazing incidence monochromator.[13] The energy resolution for photoabsorption measurement was $E/\Delta E = 2000-4000$ under the typical conditions with the slit widths 10 μm. High photon flux, however, was required to obtain the reliable signal−noise ratio, and hence the slit widths of the monochromator were kept at 50 μm during the experiment, which provided $\Delta E \approx 1$ eV at $h\nu = 400$ eV. The intensity of the photon beam was monitored by using a silicon photodiode (IRD AXUV-100). A conventional linear TOF mass spectrometer was mounted in the main chamber. This chamber is rotatable from −20 to +110° with respect to the linearly polarized electric vector of the primary SR beam[7] and was differentially evacuated by two 300 L/s and a 1500 L/s turbomolecular pump. The base pressure was better than 3×10^{-6} Pa. Ozone was flowed as an effusive jet at right angles to the primary photon beam. The pressure in the main chamber was kept below 10^{-3} Pa during experiment.

Ozone was prepared by discharging pure O_2 using a commercial ozonator. The mixture of ozone and oxygen was trapped on silica gel in a glass trap at −110 °C and then the residual oxygen was pumped off.[7,14] Ozone should be carefully treated because admixture of a trace of pump oil may lead to an explosion. The ozone sample was stored at −78 °C when not in use.

3. Results and Discussion

Figure 1 shows the photoabsorption spectra of ozone in the K edge region previously reported in ref 7. The ionization

10.1021/jp9904670 CCC: $18.00
Published on Web 05/29/1999

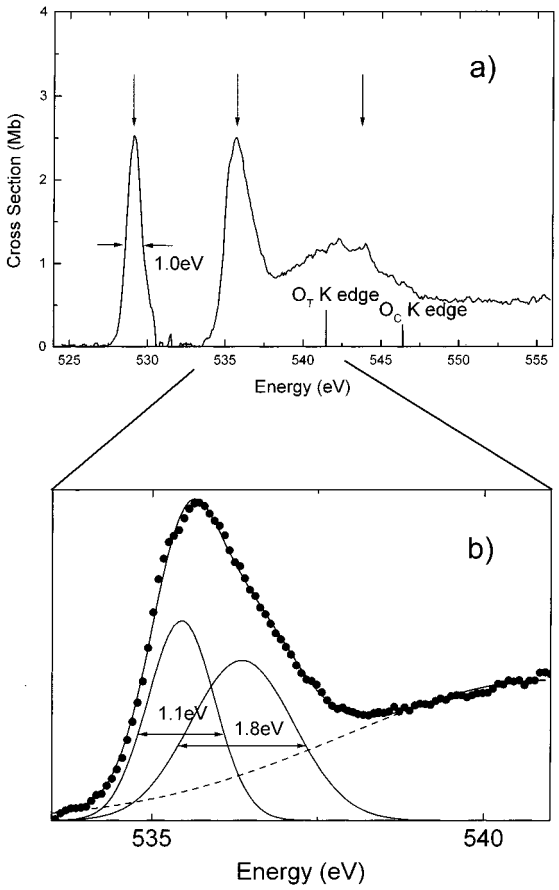

Figure 1. Photoabsorption spectrum of ozone in the K edge region. The ionization potentials of the 1s electrons are 541.5 and 546.2 eV, which are obtained by XPS of O_3.[15] Arrows show the excitation energies for the measurements of TOF spectra. The peak around 535.7 eV has been deconvoluted by several Gaussian functions. The two deconvoluted peaks have half-widths of 1.1 and 1.8 eV.

energies (IEs) for $O_T(1s)^{-1}$ and $O_C(1s)^{-1}$ of ozone have been measured to be 541.5 and 546.2 eV by XPS spectroscopy,[15] where the O_T and O_C mean the terminal and center oxygen atoms, respectively, and are indicated in Figure 1. The configuration of a molecular orbital (MO) representation in the ground-state O_3 is

$$\text{Core: } 1a_1^2 2a_1^2 1b_2^2$$

$$\text{Valence: } 3a_1^2 2b_2^2 4a_1^2 5a_1^2 3b_2^2 1b_1^2 1a_2^2 4b_2^2 6a_1^2$$

$$\text{Vacant: } 2b_1^0 7a_1^0 5b_2^0$$

where the innermost $1a_1$ MO corresponds to the 1s orbital of the central oxygen atom. The degenerate $2a_1$ and $1b_2$ MO's correspond to appropriate even (+) and odd (−) combinations of the terminal O(1s) orbitals, respectively.

The TOF mass spectra were measured at 529.0, 535.7, and 544.6 eV, shown by arrows in Figure 1, for the $\pi^*(2b_1) \leftarrow O_T(1s)$, $\pi^*(2b_1) \leftarrow O_C(1s)/\sigma^*(7a_1) \leftarrow O_T(1s)$, and $\sigma^* \leftarrow O_C(1s)$ transitions, respectively.[7] The detector axis was set at 0° (denoted as "horizontal") or 90° (denoted as "vertical") with respect to the linearly polarized synchrotron radiation. Figure 2 shows the vertical TOF spectra at the excitation energy 529.0 eV. The products observed were O_3^+, O_2^+, O^+, O_2^{2+}, and O^{2+}. The contribution from the oxygen molecule is inevitable because oxygen made up ≈60% of the O_3 sample.[7] Note in Figure 2b that the O_2^+ peak arising from the pure O_2 molecule has no tail

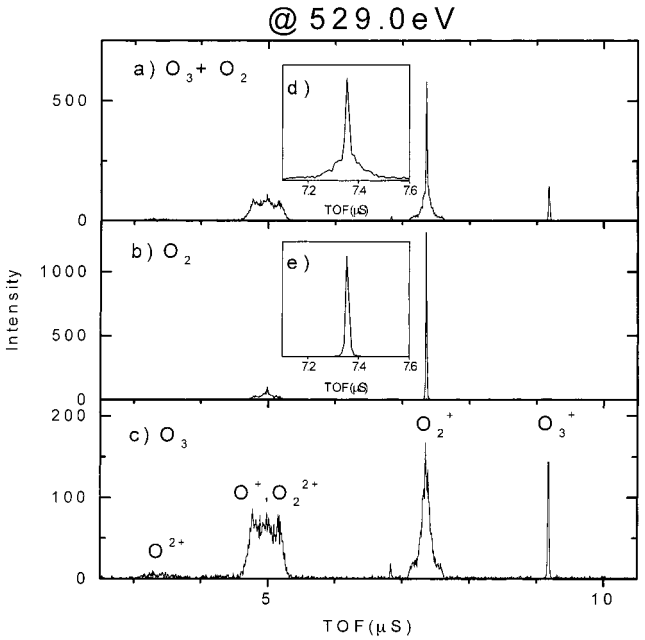

Figure 2. TOF spectra of (a) a mixture of O_2 and O_3 and (b) pure O_2. The spectrum of (c) O_3 was obtained by subtraction of these two spectra, assuming that the center part of peak in the mixture is composed of only O_2 spectra. (d) and (e) show the O_2^+ TOF spectra, which indicates that the narrow O_2^+ part at 7.35 μs arises from pure O_2.

and gives the narrow band since it has no kinetic energy released. The corrected spectrum for O_3 in Figure 2c was obtained after removal of the contribution from the coexisting O_2 component on the assumption that the sharp band at 7.35 μs originates in pure O_2 (see Figure 2d,e).

Figure 3 shows the TOF spectra at the vertical and horizontal positions excited at 529.0, 535.7, and 544.6 eV. In these spectra, the contribution from O_2 was subtracted by the procedure mentioned above. At the excitation energy 529.0 eV, the O^+ ion ejected to the vertical direction consists of three peaks with local maxima: The center one is presumably due to O^+ and O_2^{2+} with no kinetic energy. Two wing peaks should be O^+ fragments. On the other hand, the energy distribution obtained from the ions at the horizontal position shows the relatively narrow single O^+ peak. The difference of these two shapes arises from the fact that the O^+ fragment is preferably emitted to the vertical direction with some kinetic energy. Since the geometry of ozone in the ground state is bent (C_{2v}), this is consistent with our previous assignment that the 529 eV band is the $\pi^*(2b_1) \leftarrow 1s(2a_1)$ transition, whose transition moment lies perpendicular to the C_{2v} molecular plane. In contrast to this, at an excitation energy of 535.7 eV, the O^+ ion ejected both to the vertical and to the horizontal direction consists of three peaks. This implies that the O^+ fragment ions were ejected more isotropically.

To clarify this, we have calculated the β values and kinetic energy distribution by simulation.[8−10] Briefly, the trajectory of the fragment ion having one kinetic energy and one β value was calculated, which provides us a part of the TOF spectrums at the vertical and horizontal positions. Then, by using different kinetic ions in which weight factors were assumed for individual kinetic energies, a weighted summation of the TOF spectrum was calculated. Finally, the difference between calculated and measured TOF spectra was minimized by adjusting these weight factors and the β value.[8−10] The polarization degree of light at the photon energy of 530 eV was calculated from that observed at 65 eV.[16]

In Figure 4 and Table 1, respectively, we have shown the kinetic energy distribution and β values of O^+ and O_2^{2+}. In

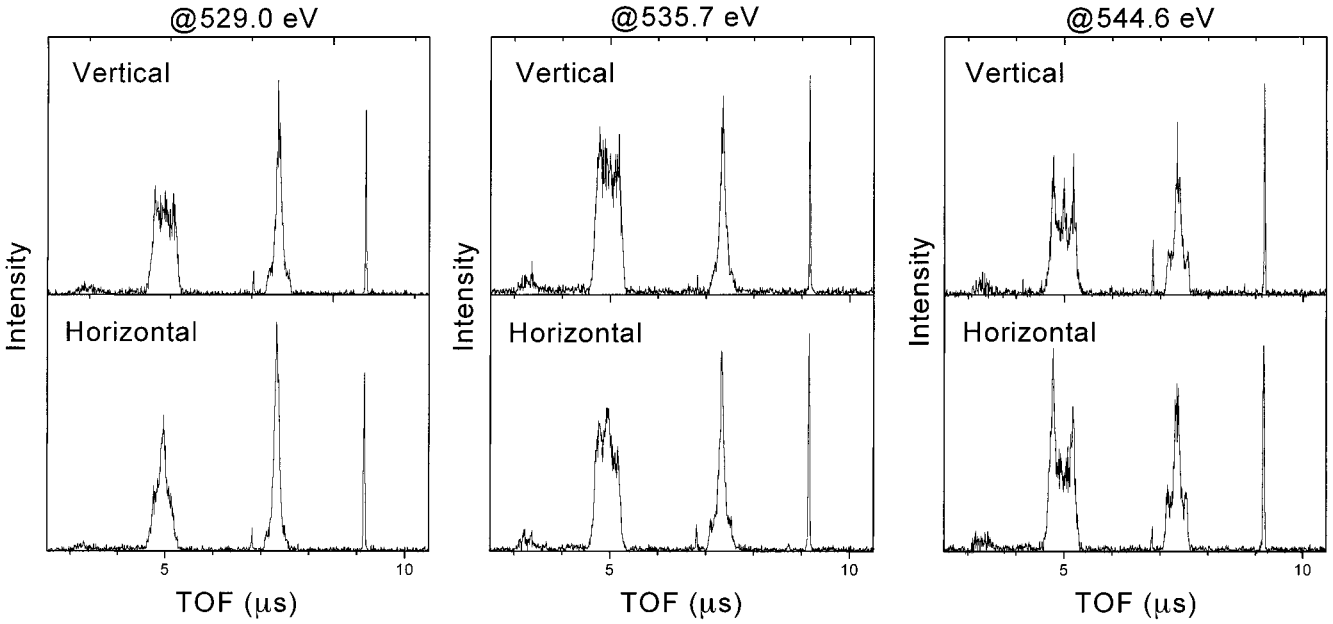

Figure 3. TOF spectra obtained when the detector is set horizontal and vertical to the direction of polarization of light. The excitation energies are 529.0, 535.7, and 544.6 eV, which correspond to positions of the arrows in Figure 1.

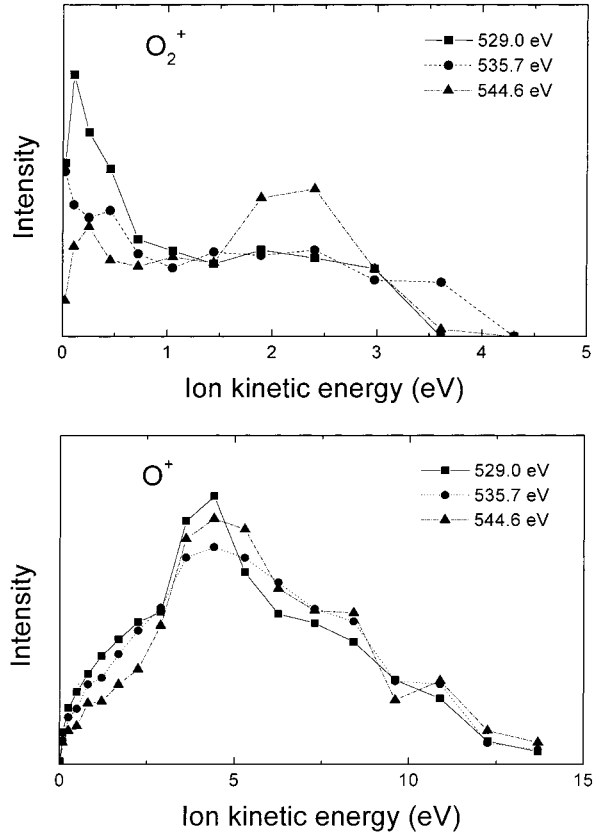

Figure 4. Kinetic energy distribution of O^+ and O_2^{2+} calculated from the TOF spectra.

Figure 4, the energy distributions slightly vary as the photon energy changes. The maximum is seen at about 4 eV. The kinetic energy distribution of O^+ from O_2 excited to same K edge region (530−546 eV) shows a maximum at 5−6 eV,[8] which is higher than that of ozone. Table 1 shows the relatively small β value of O_2^+ compared with O^+. On the basis of large contamination by the oxygen molecule, this may be due to the large effect of ions from oxygen, although we have subtracted it in the calculation.

TABLE 1: β Values of Ion Photofragments Observed at Three Energies

	529.0 eV	535.7 eV	544.6 eV
O^+	−0.7	−0.3	0.4
O_2^+	−0.2	0.0	0.1

The β value of O^+ at an excitation energy of 529.0 eV is −0.7, which is consistent with our previous assignment that the 529 eV band comes from the $\pi^*(2b_1) \leftarrow 1s(2a_1)$ transition. Deviation from the predicted value of −1 for the pure $\pi^*(2b_1) \leftarrow 1s(2a_1)$ transition may arise from the contribution of O_2^{2+} or an effect of the three-body dissociation process. In contrast to this, the β value at an excitation energy of 535.7 eV is −0.3. This implies that the transition moment does not lie perpendicular to the molecular plane as does the 529.0 eV excitation and that this band should be mixed by more than two transitions. This is consistent with the SCF calculation,[7] in which the $\pi^*(2b_1) \leftarrow O_C(1s)$ transition falls on the $\sigma^*(7a_1) \leftarrow O_T(1s)$ excitation.

If we assume that the peak around 535.7 eV mainly consists of these two transitions, the intensity ratio of these two transitions can be obtained from the β value as follows: The $\pi^*(2b_1) \leftarrow O_C(1a_1)$ transition, whose transition moment lies perpendicular to the C_{2v} molecular plane, results in the fragmentation with $\beta = -1$. The degenerated $2a_1$ and $1b_2$ MO's are almost even and odd combinations of the terminal O(1s) atomic orbitals. Assuming that ozone dissociate with the same geometry in the ground state (bend angle is 117°) and two transitions, $\sigma^*(7a_1) \leftarrow O_T(2a_1$ and $1b_2)$, have the same intensities, these transitions are expected to result in the fragmentation with $\beta = 0.5$. The observed β value, β', is expressed as[17,18]

$$T = T_1 + T_2$$

$$x = T_1/T$$

$$\beta' = x\beta_1 + (1 - x)\beta_2$$

where T_1 and T_2 are the transition probability of $\pi^*(2b_1) \leftarrow O_C(1a_1)$ and $\sigma^*(7a_1) \leftarrow O_T(2a_1$ and $1b_2)$, respectively. β_1 and β_2 are β values for the $\pi^*(2b_1) \leftarrow O_C(1a_1)$ and $\sigma^*(7a_1) \leftarrow O_T$-

TABLE 2: Branching Ratios of Ion Photofragments Observed at Three Energies[a]

	529.0eV (%)	535.7eV (%)	544.6eV (%)
O_3^+	8 ± 1 (∥), 6 ± 1(⊥)	8 ± 1, 5 ± 1	7 ± 1, 8 ± 1
O_2^+	42 ± 2, 37 ± 3	30 ± 3, 25 ± 3	33 ± 2, 32 ± 3
O^+, O_2^{2+}	46 ± 4, 54 ± 2	58 ± 2, 63 ± 3	54 ± 5, 55 ± 4
O^{2+}	4 ± 2, 5 ± 2	5 ± 1, 6 ± 1	5 ± 1, 5 ± 1

[a] Left values were measured when the polarization is set to horizontal position (∥), while right ones were measured when it is set to vertical position (⊥).

($2a_1$ and $1b_2$) transitions, respectively. Therefore, the ratio of transition probability, T_1:T_2, can be calculated to be 1:0.88.

This is consistent with the analysis of the absorption band observed: We have deconvoluted the peak at 535.7 eV by three Gaussian functions (Figure 1b). At 535.7 eV, the intensity ratio of these two strong Gaussian bands are 1:0.65, which is close to the above value. Half-widths of these two Gaussian functions are 1.1 and 1.8 eV, as seen in Figure 1b. Since two peaks at 529.0 and 535.7 eV have similar bandwidths, 1.0 and 1.1 eV, this agreement also supports that two bands arise from the same final state, π^* state. We should note that there is ambiguity of these values, especially, the number of Gaussian functions: for example, four or five Gaussian functions can be fitted to the absorption band, although we have chosen three as the simplest case.

Table 2 shows the appearance of fragments O_3^+, O_2^+, and O^+ and O^{2+} depending on the excitation energies. The main products observed were O_2^+ and O^+. Those fragments account for 85−90% of products for these excitation energies. The parent O_3^+ was also produced. However, it is less than 8% of total ions. In Table 2 the fragment distributions are similar in the excitations of center O(1s) electrons at 535.7 and 544.6 eV, which means the effect of excitation energy on the fragmentation is not considerable. On the contrary, the O_2^+ fragment is preferably formed at the $\pi^*(2b_1) \leftarrow O_T(1s)$ excitation, especially 42% at the horizontal experiment. This enhancement of O_2^+ can be attributed to the atomic site selectivity of the relaxation processes following the initial excitation. That is, the core hole associated with the terminal oxygen produces the large yield of molecular O_2^+ fragment ion.

A similar Auger decay process had been observed for N_2O,[2,19] in which the relaxation mechanism following the terminal nitrogen excitation produces the largest yield of molecular ions (N_2^+ and NO^+). Recently, Ferrand-Tanaka et al. have found that the N_t-N_c bond is preferentially broken when the Auger electrons from the 2π state are observed.[19] In view of this, it is very important to observe the Auger electron spectra of the ozone and, as a result, to reveal the resonant Auger process of the K shell excited state. As far as we know, however, there exists no information about the resonant Auger process of ozone.

4. Conclusions

The photodissociation of ozone in the K edge region has been investigated by time-of-flight spectra of ion photofragments. By using the angle-resolved time-of-flight method, the β values and translational energy distributions of fragments were calculated. It shows that two excitations, $\pi^*(2b_1) \leftarrow O_C(1s)$ and $\sigma^*(7a_1) \leftarrow O_T(1s)$, are overlapped in the band. A π^* excitation from the inner 1s of the terminal oxygen atoms generates preferably O_2^+, compared to that from the inner 1s of the center oxygen atom.

Acknowledgment. Support of this work by New Energy and Industrial Technology Development Organization (NEDO) and Japan Science Program Society (JSPS) is gratefully acknowledged.

References and Notes

(1) Eberhardt, W.; Sham, T. K.; Carr, R.; Krummacher, S.; Strongin, M.; Weng, S. L.; Wesner, D. *Phys. Rev. Lett.* **1983**, *50*, 1038.
(2) Murakami, J.; Nelson, M. C.; Anderson, S. L.; Hanson, D. M. *J. Chem. Phys.* **1986**, *85*, 5755.
(3) Müller-Dethlefs, K.; Sander, M.; Chewter, L. A.; Schlag, E. W. *J. Phys. Chem.* **1984**, *88*, 6098.
(4) Habenicht, W.; Baiter, H.; Müller-Dethlefs, K.; Schlag, E. W. *J. Phys. Chem.* **1991**, *95*, 6774.
(5) Ueda, K.; Chiba, H.; Sato, Y.; Hayaishi, T.; Shigemasa, E.; Yagishita, A. *Phys. Rev. A* **1992**, *46*, R5.
(6) Erman, P.; Karawajczyk, A.; Rachlew, E.; Stankiewicz, M.; Franzen, K. Y. *J. Chem. Phys.* **1997**, *107*, 10827.
(7) Gejo, T.; Okada, K.; Ibuki, T. *Chem. Phys. Lett.* **1997**, *277*, 497.
(8) Saito, N.; Suzuki, I. H. *J. Chem. Phys.* **1989**, *91*, 5329.
(9) Saito, N.; Suzuki, I. H. *Int. J. Mass. Spectrom. Ion Processes* **1988**, *82*, 61.
(10) Bozek, J. D.; Saito, N.; Suzuki, I. H. *J. Chem. Phys.* **1993**, *98*, 4652.
(11) Kosugi, N.; Adachi, J.; Shigemasa, E.; Yagishita, A. *J. Chem. Phys.* **1992**, *97*, 8842.
(12) Adachi, J.; Kosugi, N.; Shigemasa, E.; Yagishita, A. *J. Chem. Phys.* **1995**, *102*, 7369.
(13) Hiraya, A.; Nakamura, E.; Hasumoto, M.; Kinoshita, T.; Sakai, K.; Ishiguro, E.; Watanabe, M. *Rev. Sci. Instrum.* **1995**, *66*, 2104.
(14) Thelen, M.-A.; Gejo, T.; Harrison, J. A.; Huber, J. R. *J. Chem. Phys.* **1995**, *103*, 7946.
(15) Banna, M. S.; Frost, D. C.; McDowell, C. A.; Noodleman, L.; Wallbank, B. *Chem. Phys. Lett.* **1977**, *49*, 213.
(16) Hatano, T.; Hu, W.; Yamamoto, M.; Watanabe, M. *J. Electron. Spectrosc. Relat. Phenom.* **1998**, *92*, 311.
(17) Frey, J. G.; Felder, P. *Mol. Phys.* **1992**, *75*, 1419.
(18) Kim, D. Y.; Lee, K.; Ma, C. I.; Mahalingam, M.; Hansen, D. M.; Hulbert, S. L. *J. Chem. Phys.* **1992**, *97*, 5915.
(19) Ferrand-Tanaka, L.; Simon, M.; Thissen, R.; Lavollee, M.; Morin, P. *Rev. Sci. Instrum.* **1995**, *66*, 1587.